

Ultrasonic Preparation of Polymer/Layered Silicate Nanocomposites during Extrusion

Jiang Li, Lijuan Zhao, Shaoyun Guo (✉)

The State Key Laboratory of Polymer Materials Engineering, Polymer Research Institute of Sichuan University, Chengdu 610065, China
Email: nic7702@scu.edu.cn; Fax:86-28-85402465

Received: 25 April 2005 / Revised version: 13 June 2005 / Accepted: 6 July 2005
Published online: 22 July 2005 – © Springer-Verlag 2005

Summary

Three kinds of polymer/layered nanocomposites were prepared via ultrasonic extrusion. Experimental results showed that ultrasonic oscillations could mostly decrease the size and its distribution of clay particles in polymer matrix. Therefore, crystal size of polymer matrix decreases. For PA6-based nanocomposites with higher compatibility, the ultrasonic oscillations can also affect the microstructure of clay, causing more regions of exfoliated clay. Due to better dispersion of clay and smaller crystal size, the elongation at break of polymer/layered nanocomposites ultrasonically treated got greatly increased, meanwhile ultrasonic oscillations also improved their other mechanical properties, such as tensile and impact strength.

Introduction

In recent years polymer/layered silicate nanocomposites (PLS) have attracted great interest, both in industry and in academia, because they often exhibit remarkable improvement in materials properties when compared with neat polymers or conventional micro- and macro-composites [1]. Intercalation of polymer in layered silicate has proven to be a successful approach to synthesize PLS nanocomposites. The preparative methods are divided into three main groups according to the processing techniques: intercalation of polymer from solution, in situ intercalative polymerization method and melt intercalation method. Comparatively, melt intercalation method has great advantages over either in situ intercalative polymerization or polymer solution intercalation. First, this method is environmentally benign due to the absence of organic solvents. Second, it is compatible with current industrial process, such as extrusion [1].

Recently, many methods were applied to prepare PLS nanocomposites with excellent properties, summarized as follows:

- (1) to synthesize novel organically modified layered silicate (OMLS) with expanded basal spacing of the silicate layers, which is useful to the intercalation of polymer in layered silicate [2-4].
- (2) to modify further the OMLS and polymer matrix in order to enhance the interfacial interaction between two phases [5-11].

(3) to optimize the preparative conditions of PLS, such as temperature, time, clay loading and molecular weight of polymer [12-15].

In general, the addition of OMLS in polymer matrix can increase the tensile and flexural modulus, yield strength compared to those of neat polymer materials [13, 16-20]. But for elongation at break or impact strength, PLS nanocomposites exhibit a small or large decrease. In case of some PA6/layered silicate nanocomposites [16], with the addition of clay in PA6, the elongation at break greatly decreases from 101% to 18% at a test rate of 5.1 cm/min due to the presence of stacked silicate layers. Therefore, a key to increase the ductility of PLS nanocomposites is to prevent the congregation of layered silicate.

Recently, ultrasonic extrusion technology, which organically combines extruder and power ultrasound, has been developed in our lab. In our previous studies, the introduction of ultrasonic irradiation in extrusion processing of polymer can not only improve the processibility of polymer materials [21], but also reduce the size and its distribution of dispersed particles in polymer blends [22, 23]. In this paper, we reported the preparation of three polymer/montmorillonite clay nanocomposites via ultrasonic extrusion technology, i.e. PA6-based, PE-based and PP-based nanocomposites, and their morphology can get increased.

Experimental

Materials and preparation

The polymer materials for preparation of PLS nanocomposites were high-density polyethylene (HDPE, 6098) and polypropylene (PP, EPS30R), supplied by Plastic Factory of Qilu Petrochemical Co, SINOPEC, China, and polyamide 6 (PA6, M23400), obtained from Xinhui Meida-DMS Nylon Chips Co., Ltd., Guangdong, China. The compatibilizers were maleic anhydride grafted high-density polyethylene (HDPE-g-MA, GPM100A) and maleic anhydride grafted polypropylene (PP-g-MA, GPM200) with MA content of 0.1wt. %, supplied by Ningbo Nengzhiguang New Materials Technology Co., Ltd.. Montmorillonite (MMT, DK1) organically modified with 16-C alkyl quaternary ammonium was supplied by Zhejiang Fenghong Clay Chemicals Co.. All materials were dried for 36 h before preparation of nanocomposites.

Polymer materials and MMT were premixed and then were fed a single-screw extruder for pelleting. The preparation of polymer/MMT nanocomposites was carried out in a special ultrasonic oscillations extrusion system developed in our lab, the schematic diagram of which is shown in Figure 1. It consists of an extruder and a cylinder die connected to a generator of ultrasonic oscillations. The maximum power output and frequency of the generator are 400 W and 20 KHz, respectively. The ultrasonic oscillations are in the direction parallel to the flow of the polymer melt. A pressure transducer and a thermocouple at the die entry were installed for continuous recording of the variation of pressure and temperature during extrusion. The extrudates were pelletized, then compression-molded into 1 mm and 4 mm thick plates by the compression molding press at a pressure of 12 MPa for 10 min, to obtain specimens for measurement and characterization. The sample codes and preparative conditions are listed in Table 1.

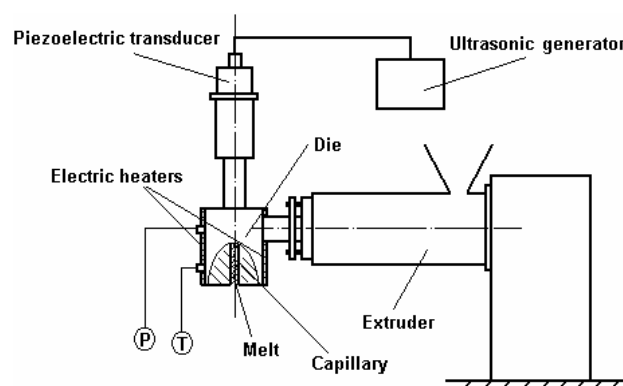


Figure 1. Schematic diagram of ultrasonic oscillations extrusion system.

Table 1. Sample codes, preparative conditions and mechanical properties.

Samples	Polymer matrix	MMT loading (wt%)	Ultrasonic intensity (W)	Yield strength (MPa)	Elongation at break (%)	Young's modulus (MPa)
PA6		0	0	29.3	276.0	685.2
PA6CN-0	PA6	3	0	36.2	19.4	1049.2
PA6CN-100		3	100	38.4	30.9	1084.3
HDPE		0	0	22.4	684.2	814.6
PECN-0 ^a	HDPE	3	0	22.5	585.9	1215.5
PECN-200 ^a		3	200	25.0	762.9	1366.3
PP		0	0	22.2	658.7	973.4
PPCN-0 ^a	PP	3	0	21.2	12.7	1299.0
PPCN-100 ^a		3	100	23.9	269.7	1614.0

^a Compatibilizer loading (wt%): 9

Measurements and Characterization

The extent of clay intercalation in the nanocomposites was determined under ambient conditions by X-ray diffraction (XRD) using a Philip X'Pert Pro MPD diffractometer (Cu K α radiation, generator voltage=40KV, current=40mA). Samples were scanned in 2θ ranges from 0.5 to 35° at a rate of 1°/min. To study the microstructure, transmission electron microscopy (TEM) micrographs were taken from ultrathin sections of the nanocomposites with a JEM-CX100 TEM, using an acceleration voltage of 100KV. A Hitachi X-650 scanning electron micrograph (SEM) made in Japan was used to investigate the morphology of dispersed phase in polymer matrix. SEM observations were made on the impact fracture surfaces at the temperature of liquid nitrogen. Gold was coated on the fractured surfaces before the SEM observations. Polarized Light Microscope (PLM) observation was measured with Leita Laborlux 12Pols made in Germany. Tensile measurements were performed at room temperature on an Instron 4302 tension machine (Canton, MA) with specimen dimension of 25mm×6.5mm×1mm and a crosshead speed of 100mm/min. Impact strength testing was conducted according to the regulation mentioned in GB1843-80 at room temperature. All the results were the average of five measurements.

Results and discussion

The change of the interlayer distance can be detected by XRD. Figure 2 shows the results of XRD patterns of both organoclay and polymer/organoclay hybrids in the range of $2\theta=1-12^\circ$. The organoclay (MMT) pattern reveals a broad intense peak around $2\theta=3.75^\circ$, corresponding to a basal spacing of 2.354nm. For polymer-based nanocomposites, their characteristic basal reflections are observed at below 3.75° (meaning $d_{(001)} > 2.354\text{nm}$), implying an intercalated structure via extrusion processing. In detail, the pattern of PECN-200, which was extruded under a 200W ultrasonic irradiation, shows an almost same basal peak around $2\theta=2.35^\circ$ ($d_{(001)} = 3.756\text{nm}$) as that of PECN-0, indicating that the ultrasonic oscillations can't affect the extent of intercalation. Similar result can be revealed by comparing the XRD patterns of PPCN-0 and PPCN-100. Their (001) plane diffraction peak appears at around $2\theta=2.42^\circ$ ($d_{(001)} = 3.648\text{nm}$). But for PA6-based nanocomposites, ultrasonic oscillations can change the intercalated structure due to higher compatibility between PA6 matrix and MMT. The PA6CN-0 XRD pattern shows a low, broad shadow peak around 2.57° of 2θ ($d_{(001)} = 3.435\text{nm}$). For PA6CN-100 ultrasonically treated, a small remnant shoulder is observed at around $2\theta=2.35^\circ$ ($d_{(001)} = 3.756\text{nm}$). The PA6CN-100 X-ray results suggest that the ultrasonic irradiation causes more regions of exfoliated MMT clay. TEM photomicrographs of PA6CN-0 and PA6CN-100, shown in Figure 3, further prove the effect of ultrasonic irradiation on PA6-based nanocomposites microstructure. The TEM bright field image of PA6CN-0, Figure 3a, shows an intercalated structure, where the stacked silicate layers are observed. The PA6CN-100 photomicrograph indicates that the ultrasonic oscillations cause partial exfoliation with areas containing exfoliated platelets and areas of intercalated structure.

On the other hand, SEM observation, shown in figure 4, can reveal the morphology of PP-based nanocomposites. The SEM image of PPCN-0 shows the stacked clay particles with much higher size and size distribution compared to that of PPCN-100,

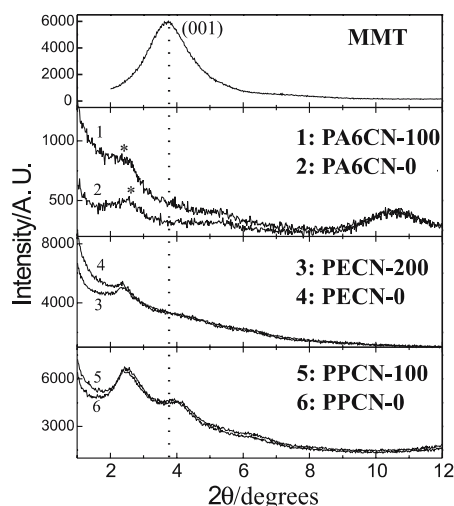


Figure 2. WAXD patterns for MMT and polymer/MMT clay hybrids. The dashed lines indicate the location of the silicate (001) reflection of MMT. The asterisks indicate a remnant shoulder for PA6CN-100 or a small peak for PA6CN-0.

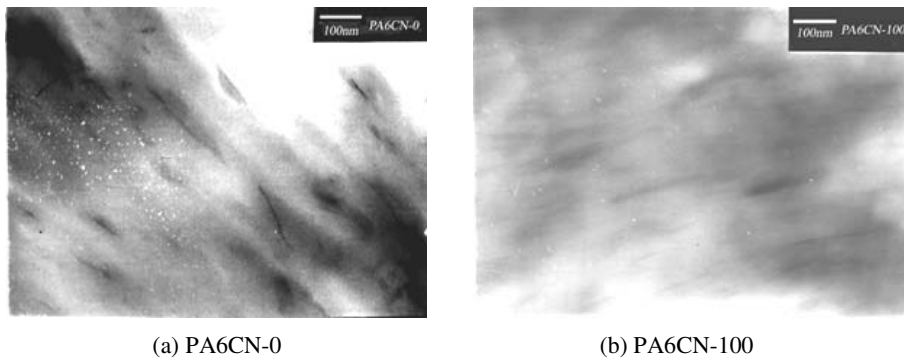


Figure 3. TEM micrographs showing PA6CNs for (a) PA6CN-0 and (b) PA6CN-100. The dark lines are the cross-sections of MMT layers and the bright areas are the PA6 matrix.

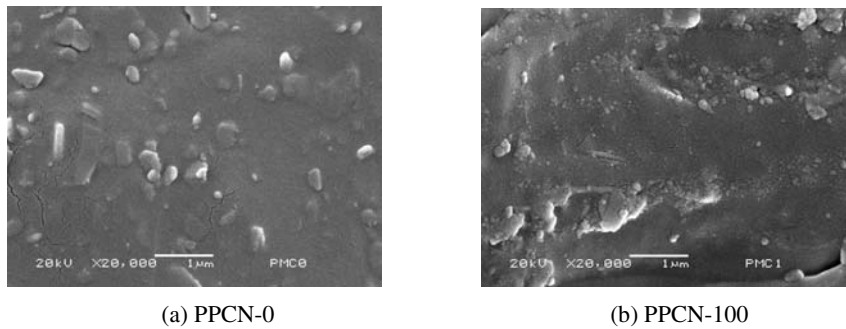




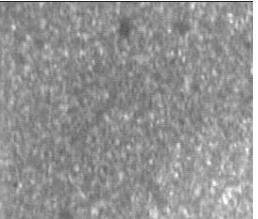
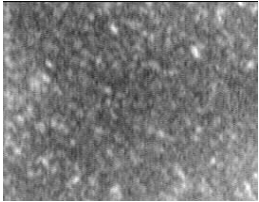
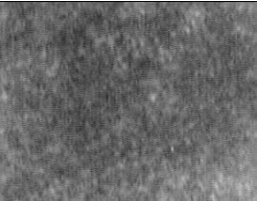
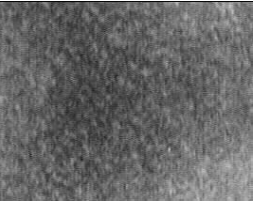
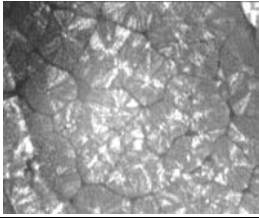
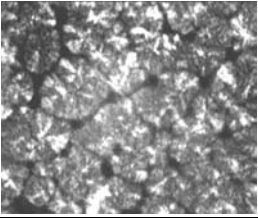
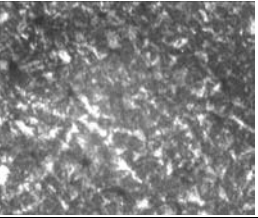
Figure 4. SEM micrographs for (a) PPCN-0 and (b) PPCN-100.

which was treated with 100 W ultrasonic oscillations. This indicates that the ultrasound can obviously prevent the agglomeration of clay and improve the dispersion of clay in polymer matrix.

Particles of MMT have heterogeneous nucleation effects on polymer matrix. The decrease of size of MMT particles, caused by ultrasonic treatment, would affect the crystalline behavior of polymer matrix. The PLM data and figures showed in Table 2 indicate that the addition of MMT into polymers shortens induction time of crystallization and decrease crystal size. Ultrasonic treatment further enhances these changes.

The mechanical properties of pure polymers and polymer/organoclay hybrids are shown in Table 1. It can be found that the addition of MMT into polymers greatly increase Young's modulus, but decrease elongation at break. In comparison to the nanocomposites untreated with ultrasonic irradiation, the yield strength and Young's modulus of ultrasonically treated nanocomposites have been improved with great increase of elongation at break. In general, the addition of clay in polymer matrix causes a decrease of ductility, even a fragile fracture with high clay loading. In our experiments, the ultrasonic oscillations overcame this disadvantage meanwhile increasing other mechanical properties. For PA6CN-100, PECN-200 and PPCN-100, the elongation at break of increases by 58.9%, 30.2% and substantial 1960.9%,

Table 2. The effects of MMT and ultrasonic treatment on crystalline behavior of polymer matrix.

Samples	PA6	PA6CN-0	PA6CN-100
Induction period (s)	40-50	10-20	Less than 10
PLM photos (×500) Crystallizing temperature 195 °C			
Samples	HDPE	PECN-0	PECN-200
Induction period (s)	50-60	40-50	30-40
PLM photos (×500) Crystallizing temperature 122 °C			
Samples	PP	PPCN-0	PPCN-100
Induction period (s)	40-50	10-20	Less than 10
PLM photos (×500) Crystallizing temperature 130 °C			

respectively, compared to that of hybrids untreated with ultrasonic irradiation. This attributes to the better dispersion of clay and smaller crystal size induced by ultrasonic oscillations, just as already seen in the SEM and PLM results.

Acknowledgements. The authors are grateful to the Special Funds for Major State Basic Research Projects of China (G1999064800), National Natural Science Foundation of China (50233010, 20374037) financial support of this work.

References

1. Suprakas Sinha Ray, Masami Okamoto (2003) *Progress in Polymer Science* 28: 1539
2. Fornes TD, Yoon PJ, Hunter DL, Keskkula H, Paul DR (2002) *Polymer* 43: 5915
3. Gilman JW, Awad WH, Davis RD, Shields J, Trulove PC, DeLong HC (2002) *Chemistry of Materials* 14: 3776

4. Maiti P, Yamada K, Okamoto M, Ueda K, Okamoto K (2002) *Chemistry of Materials* 14: 4654
5. Kawasumi M, Hasegawa N, Kato M, Usuki A, Okada A (1997) *Macromolecules* 30: 6333
6. Hasegawa N, Kawasumi M, Kato M, Usuki A, Okada A (1998) *Journal of Applied Polymer Science* 67: 87
7. Pham Hoai Nam, Pralay Maiti, Masami Okamoto, Tadao Kotaka, Naoki Hasegawa, Animitsu Usuki (2001) *Polymer* 42: 9633
8. Xiaohui Liu, Qiuju Wu (2001) *Polymer* 42: 10013
9. Ki Hyum Wang, Min Ho Choi, Chong Min Koo, Yeong Suk Choi, In Jae Chung (2001) *Polymer* 42: 9819
10. Lu HL, Hong S, Chung TC (1998) *Macromolecules* 31: 2028
11. Bing Lu, Chung TC (2000) *Journal of Polymer Science Part A: Polymer Chemistry* 38: 1337
12. Vaia RA, Ishii H, Giannelis EP (1993) *Chemistry of Materials* 5: 1694
13. Fomes TD, Yoon PJ, Keskkula H, Paul DR (2001) *Polymer* 42: 9929
14. Cher H Davis, Lon J Mathias, Jeffrey W Gilman, David A Schiraldi, J Randy Shields, Paul Trulove, Tom E Sutto, Hugh C Delong (2002) *Journal of Polymer Science Part B: Polymer Physics* 40: 2661
15. Bing Liao, Mo Song, Haojun Liang, Yongxin Pang (2001) *Polymer* 42: 10007
16. Kojima Y, Usuki A, Kawasumi M, Okada A, Kurauchi T, Kamigaito O (1993) *Journal of Polymer Science Part A: Polymer Chemistry* 31: 1755
17. Nam PH, Maiti P, Okamoto M, Kotaka T (2001) *Proceeding Nanocomposites. ECM Publication, Chicago Illinois USA*
18. Suprakas Sinha Ray, Kazunobu Yamada, Masami Okamoto, Kazue Ueda (2003) *Polymer* 44: 857
19. Wang Z, Lan T, Pinnavaia TJ (1996) *Chemistry of Materials* 8: 2200
20. Ang-Rock Lee, Hwan-Man Park, Hyuntaek Lim, Taekyu Kang, Xiucuo Li, Won-Jei Cho, Chang-Sik Ha (2002) *Polymer* 43: 2495
21. Guangshun Chen, Shaoyun Guo, Huilin Li (2002) *Journal of Applied Polymer Science* 84: 2451
22. Guangshun Chen, Shaoyun Guo, Huilin Li (2002) *Journal of Applied Polymer Science* 86: 23
23. Jiang Li, Mei Liang, Shaoyun Guo, Vanda Kuthanová, Berenika Hausnerová (2005) *Journal of Polymer Science Part B: Polymer Physics* 43: 1260